

University of Groningen

Low Driving Voltage and High Mobility Ambipolar Field-Effect Transistors with PbS Colloidal Nanocrystals

Bisri, Satria Zulkarnaen; Piliego, Claudia; Yarema, Maksym; Heiss, Wolfgang; Loi, Maria Antonietta

Published in:
Advanced materials

DOI:
[10.1002/adma.201205041](https://doi.org/10.1002/adma.201205041)

IMPORTANT NOTE: You are advised to consult the publisher's version (publisher's PDF) if you wish to cite from it. Please check the document version below.

Document Version
Publisher's PDF, also known as Version of record

Publication date:
2013

[Link to publication in University of Groningen/UMCG research database](#)

Citation for published version (APA):

Bisri, S. Z., Piliego, C., Yarema, M., Heiss, W., & Loi, M. A. (2013). Low Driving Voltage and High Mobility Ambipolar Field-Effect Transistors with PbS Colloidal Nanocrystals. *Advanced materials*, 25(31), 4309-4314. <https://doi.org/10.1002/adma.201205041>

Copyright

Other than for strictly personal use, it is not permitted to download or to forward/distribute the text or part of it without the consent of the author(s) and/or copyright holder(s), unless the work is under an open content license (like Creative Commons).

The publication may also be distributed here under the terms of Article 25fa of the Dutch Copyright Act, indicated by the "Taverne" license. More information can be found on the University of Groningen website: <https://www.rug.nl/library/open-access/self-archiving-pure/taverne-amendment>.

Take-down policy

If you believe that this document breaches copyright please contact us providing details, and we will remove access to the work immediately and investigate your claim.

Downloaded from the University of Groningen/UMCG research database (Pure): <http://www.rug.nl/research/portal>. For technical reasons the number of authors shown on this cover page is limited to 10 maximum.

Low Driving Voltage and High Mobility Ambipolar Field-Effect Transistors with PbS Colloidal Nanocrystals

Satria Zulkarnaen Bisri,* Claudia Piliago, Maksym Yarema, Wolfgang Heiss, and Maria Antonietta Loi*

Semiconducting colloidal nanocrystals (NCs) demonstrate strong size dependency of their optical and electronic properties due to the quantum confinement of the electronic wavefunctions.^[1,2] Therefore they are promising candidates for fabrication of thin-film-based “eco-friendly” compact and power-efficient optoelectronic devices. Their colloidal nature make them ideal for solution-process fabrication. Lead-sulfide (PbS) NCs are one of the rising material stars especially because of their application in solar cells,^[3–5] photodetectors,^[6–8] as well as light-emitting devices in the near-infrared region.^[9] While the PbS NCs-based solar cell research has shown promise to achieve high power conversion efficiency, there is still a lack of understanding on the fundamental mechanism of the charge carrier transport in the assembly of these materials. Recently, there have been reports suggesting that charge carrier transport in PbS NC photovoltaic devices might have a delocalized band-like transport character despite the isolated nature of the nanocrystals.^[4] However, these findings derived from spectroscopic studies and from the fitting of the mobility from low temperature *I*–*V* characteristics of photovoltaic cells,^[4,10] therefore the data need to be confirmed by more robust transport measurements, such as those performed in a field-effect transistor configuration.

PbS NCs are still rarely used for transistor-based applications. The reason is that charge carrier mobility values in thin films of NCs are still low in comparison to their bulk material, as well as in respect to recently emerged competing solution-processed organic semiconductors.^[11,12] The molecular ligands that make NCs soluble in organic solvents behave as insulators and suppress the charge carrier transport in NC films. Most efforts to increase charge mobility in nanocrystal films consist in replacing the insulating ligands with shorter ones.^[3,13–15] Furthermore, several chemical post-deposition treatments have been reported to vary doping levels or to fill charge carrier traps in already assembled NC films.^[16,17] These techniques enhance the mobility of one charge carrier type, but suppress the other.

Therefore, despite these chemical treatments, the performances reported until now are still low, with the highest mobility being in the order of $10^{-1} \text{ cm}^2 \text{ V}^{-1} \text{ s}^{-1}$ for electron.^[18] Not enough efforts have been made to improve both charge carrier mobilities in nanocrystal thin films, by exploiting the nature of the transistor as an interfacial device.

In this communication, we report ambipolar field-effect transistors of PbS nanocrystals with very high mobility values for both charge carriers. A systematic investigation of charge carrier transport has been carried out in order to optimize the device performance. The strategy to improve charge carrier injection and to increase the density of the accumulated charge carrier has been implemented as following. Firstly, the best molecule for the ligand exchange treatment has been selected; secondly, the carrier mobility dependency on the number of percolation paths in the nanocrystal film is evaluated. Then, the influence of the metal electrode configuration on the injection properties of holes and electron has been investigated, taking in account of its position relatively to the gate dielectric. Finally, an electric-double-layer (EDL) gate of ionic-liquid-based ion gel is used in order to induce very high accumulation of charge carriers. The EDL gate technique using ionic liquid has been known to promote many field-induced phase transitions, since the probed properties of the material became more intrinsic and charge traps related with device structure are suppressed.^[19–21] This communication marks the first time ionic-liquid-based ion gel is used for PbS nanocrystal transistors. The combination of device structure optimization and use of the EDL gating is found to increase charge carrier mobilities in PbS NC transistors by almost 5 orders of magnitude, reaching $1.91 \text{ cm}^2 \text{ V}^{-1} \text{ s}^{-1}$ at 1.5 V driving voltage for electron mobility and $0.15 \text{ cm}^2 \text{ V}^{-1} \text{ s}^{-1}$ for hole mobility.

The ambipolar FETs are fabricated using the layer-by-layer (LbL) sequential spin-coating technique (Figure 1a). To replace the native oleic acid (OA) ligand, a ligand exchange procedure is performed after the deposition of each layer. This process allows, at the same time, the cross-linking of the NC film, making it possible the deposition of the next layer.^[4] For the fabrication of all FETs described in this work, PbS NCs with absorption peak of $\lambda = 1104 \text{ nm}$, energy gap $E_g = 1.12 \text{ eV}$ and a diameter $d = 3.6 \text{ nm}$ (Figure 1b) are used. Three different molecular ligands were tested, namely benzenedithiol (BDT), ethanedithiol (EDT), and 3-mercaptopropionic acids (3MPA). BDT molecules have been shown to be effective in crosslinking PbS NCs due to the two symmetric thiol end groups. Solar cells fabricated using BDT-crosslinked PbS NCs have demonstrated high efficiency and the signature of band-like transport.^[3,4] The shorter EDT molecule also has two thiol-anchoring-groups

Dr. S. Z. Bisri, Dr. C. Piliago, Prof. M. A. Loi
Zernike Institute for Advanced Materials
University of Groningen
Nijenborgh 4, 9747 AG Groningen, The Netherlands
E-mail: s.z.bisri@rug.nl; m.a.loi@rug.nl
Dr. M. Yarema, Prof. W. Heiss
Institute for Semiconductor and Solid State Physics
University of Linz
Altenbergerstrasse 69, Linz 4040, Austria



DOI: 10.1002/adma.201205041

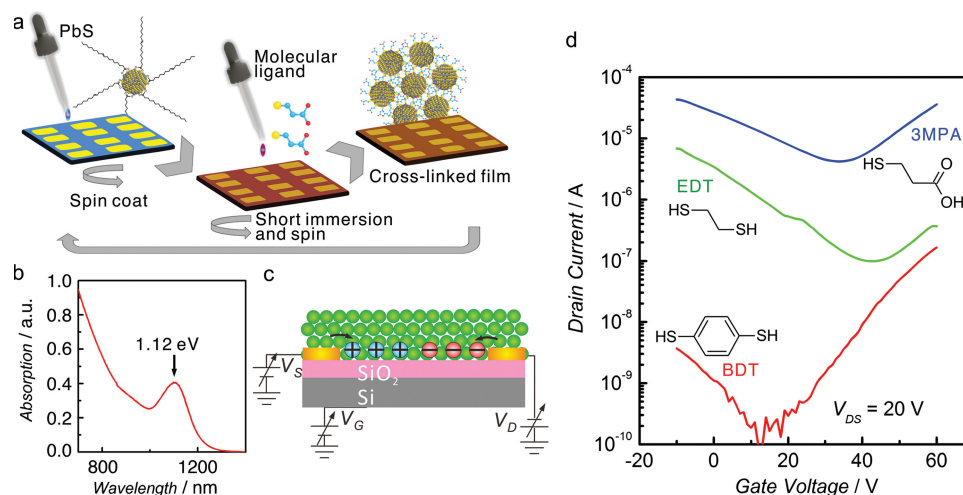


Figure 1. (a) A schematic of the layer-by-layer assembly of the colloidal nanocrystal film. (b) Absorption spectrum of the PbS colloidal nanocrystal in chloroform solution. (c) Schematic of ambipolar transistor of colloidal nanocrystals. (d) Comparison of I_D - V_G transfer curve of the colloidal nanocrystals transistors functionalized with different molecular ligands.

and recently has been used to realize ambipolar FET of PbS NCs.^[22] The carboxylate group at one end of 3MPA has been shown to have affinity for the surface of the PbS NCs.^[23] Nevertheless, the effect of these three ligands on the performance of PbS NC-based field effect transistors has never been directly compared.^[3,22,23]

At first we compared PbS NC thin film transistors (Figure 1c) treated with the three different ligands (BDT, EDT, and 3MPA) described above. Figure 1d shows the I_D - V_G transfer characteristics of the ambipolar FETs fabricated with 5-monolayer PbS NC films with different molecular ligands. All the devices exhibited ambipolar transport characteristics. However, different tendencies in charge carrier accumulation are observed. BDT-treated transistors shows the lowest drain current and the electron accumulation is better than the hole accumulation. Instead, weaker electron accumulation is obtained in EDT-treated device, although this device displays a much higher drain current than the BDT-treated device. 3MPA treatment provides a more balanced hole and electron accumulation with the highest drain current level and the lowest on/off ratio.

Quantitatively, charge carrier mobilities were obtained from the linear regime of the transport characteristics of the transistors using the following formula:

$$\mu_{lin} = \frac{L_C}{W_C V_{DS} C} \cdot \frac{\partial I_D}{\partial I_G} \quad (1)$$

BDT-treated PbS film reveal mobility values as high as $3.8 \times 10^{-5} \text{ cm}^2 \text{ V}^{-1} \text{ s}^{-1}$ and $1.8 \times 10^{-5} \text{ cm}^2 \text{ V}^{-1} \text{ s}^{-1}$ for holes (μ_h) and electrons (μ_e), respectively. Similarly to what was reported by other authors,^[22] the EDT-treated PbS transistor achieved μ_h of $1.7 \times 10^{-3} \text{ cm}^2 \text{ V}^{-1} \text{ s}^{-1}$. The obtained μ_e was $2.3 \times 10^{-4} \text{ cm}^2 \text{ V}^{-1} \text{ s}^{-1}$, is higher than the value reported for EDT-treated PbS NC transistor using a PEO/LiClO₄ polyelectrolyte gel gate.^[23] Since a polyelectrolyte gel gate accumulates much higher carrier density than conventional SiO₂ gate by filling the available traps, we attributed the higher value of electron mobility to either the better quality of the nanocrystal or the air-free layer-by-layer

deposition process that allows a lower trap density in the NC film. 3MPA-treated PbS transistors reveals better ambipolar transport in comparison to the devices treated with either BDT or EDT. μ_h and μ_e up to $2.7 \times 10^{-3} \text{ cm}^2 \text{ V}^{-1} \text{ s}^{-1}$ and $1.4 \times 10^{-2} \text{ cm}^2 \text{ V}^{-1} \text{ s}^{-1}$ are obtained, respectively. To our knowledge, these mobility values are the highest reported for 3MPA-treated PbS NC transistors. These values are achieved in transistors made on a SiO₂ dielectric, without any further surface treatment of either the dielectric^[23,24] or the NCs.^[13] Therefore, we use the 3MPA-treated PbS NC ambipolar FET as a model system to improve the performance by modifying the structure of the device. Field-effect transistors are interfacial devices, in which the semiconductor/insulator interface plays a substantial role in the charge transport and the semiconductor/metal-electrode interface influences the charge injection. Thus, in addition to the properties of the semiconducting channel material, the configuration of the transistor will determine the device performance. Most of the reported NC FETs used a coplanar bottom-gate bottom-contact (BG/BC) configuration (Figure 2a), since their fabrication process is straightforward.^[10,15,25] Except for few exceptions,^[22] there have been no systematic studies on NC FET performance with different device architectures. Therefore, we compared the performance of the ambipolar FETs made with 3MPA-treated PbS NCs in bottom-gate bottom-contact (BG/BC) to the one of the same film in staggered bottom-gate top-contact (BG/TC) configuration (Figure 2b).

Figure 2c compares the I_D - V_G transfer characteristics of the transistors with the BG/BC- and the BG/TC-configurations. The I_D values are normalized to accommodate the difference determined by the channel dimension. The most striking difference is the lower value of threshold voltage (V_{Th}) for electron accumulation in the BG/TC device than in the BG/BC device. The difference can be as much as 20 V. The two configuration do not show significant difference in the value of V_{Th} for hole accumulation. Moreover, only a slight improvement of the carrier mobilities is noticed: $3.1 \times 10^{-3} \text{ cm}^2 \text{ V}^{-1} \text{ s}^{-1}$ for μ_h and $3.8 \times 10^{-2} \text{ cm}^2 \text{ V}^{-1} \text{ s}^{-1}$ for μ_e in BG/TC; compared with

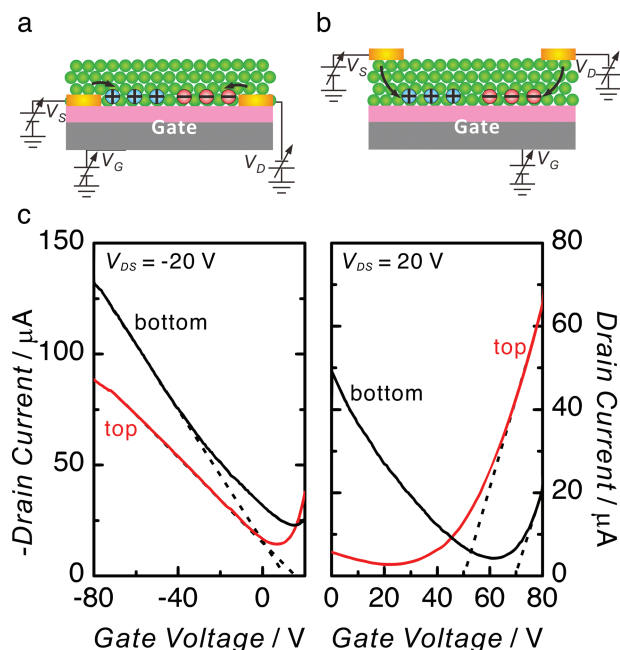


Figure 2. Schematics of charge carrier injection in (a) an in-plane bottom contact transistor configuration, and in (b) in a staggered top contact transistor configuration. (c) Comparison of the p-channel (left) and n-channel (right) I_D - V_G transfer characteristics between transistor using bottom contact configuration (black curves) and the one using top contact configuration (red curves).

$2.7 \times 10^{-3}\text{ cm}^2\text{ V}^{-1}\text{ s}^{-1}$ for μ_h and $1.4 \times 10^{-2}\text{ cm}^2\text{ V}^{-1}\text{ s}^{-1}$ for μ_e in BG/BC configuration. Since the capacitance of the oxide dielectric and their surface cleaning treatment were identical for both device structures, we consider that the difference in the V_{Th} values is mostly influenced by the position of the contact electrodes rather than by the semiconductor/insulator interface properties. It is known in organic FETs that coplanar electrode configuration becomes more resistive when higher gate voltage is applied. Moreover, carrier injection by staggered electrodes is not contact limited.^[26–29] In this study, the electron transport in SiO_2 -gated ambipolar FETs suffers of higher V_{Th} in comparison with the hole transport, because of the influence of the hydroxyl-groups which trap electrons. Consequently, higher gate voltage is necessary to have consistent electron transport. However, this high gate voltage makes the transistor to enter in a regime where contact-limited carrier injection occurs. The staggered electrode configuration leads to a minimum value of contact resistance at higher gate voltage, resulting in a lower V_{Th} for electron accumulation. Meanwhile, the V_{Th} value for hole accumulation was already low, even in the coplanar configuration, so an application of a high gate voltage is not necessary. The staggered configuration consequently does not give any significant difference around the regime where the hole accumulation starts. Nevertheless, the staggered device configuration is more beneficial for ambipolar transistors since it allows lower V_{Th} for the charge carrier type, electron, which is more likely to be trapped.^[30] Another advantage in using the BG/TC transistor configuration is the possibility to investigate the influence of the number of NC monolayers on the transport properties of the film. In the BG/BC configuration, it is

only possible to deposit up to 5 monolayers on the substrate before the contact electrodes became not visible and therefore inaccessible for measurement. In the BG/TC, we varied the number of NC monolayers (ML) from 2 up to 10 MLs, before the thermal evaporation of the Au electrodes. Figure 3a shows

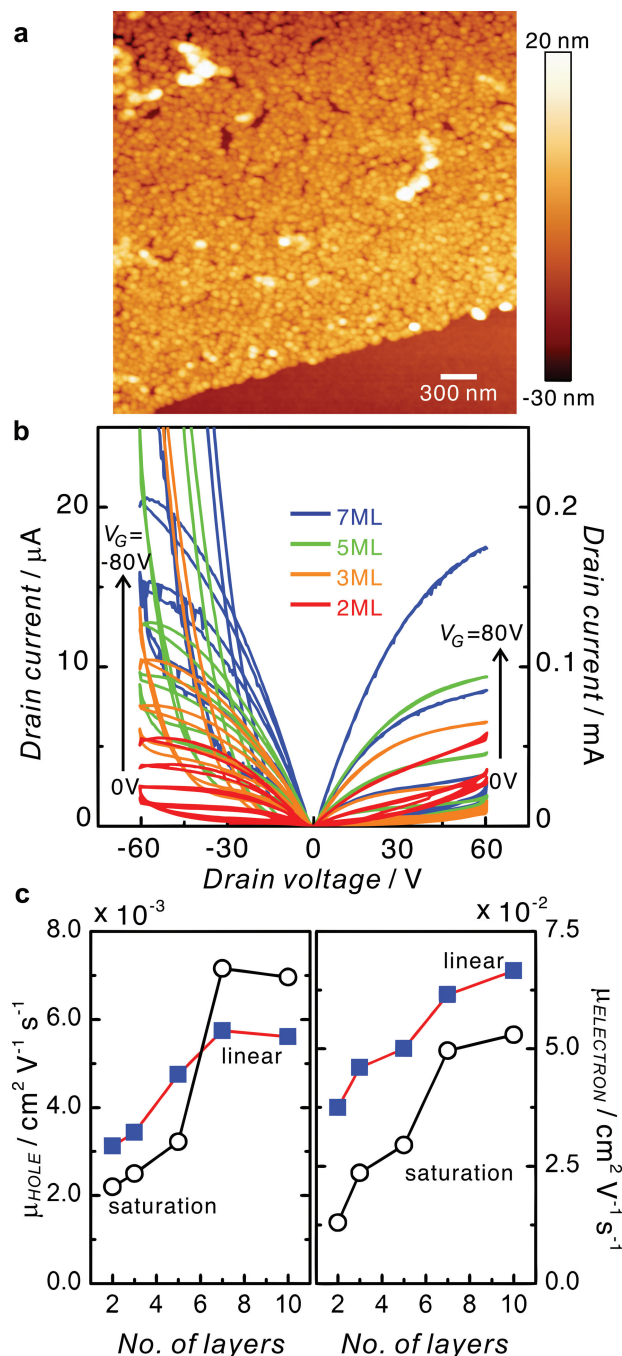


Figure 3. (a) Atomic force microscopy (AFM) image of 2-monolayers PbS nanocrystals after ligand exchange with 3-mercaptopropionic acid (3MPA), some regions of the film were intentionally removed for thickness measurement. (b) Comparison of the I_D - V_D output characteristics of top-contact ambipolar FETs using different number of nanocrystal layers. (c) Thickness-dependent mobility values for hole and electron taken in different regimes of transistor operation.

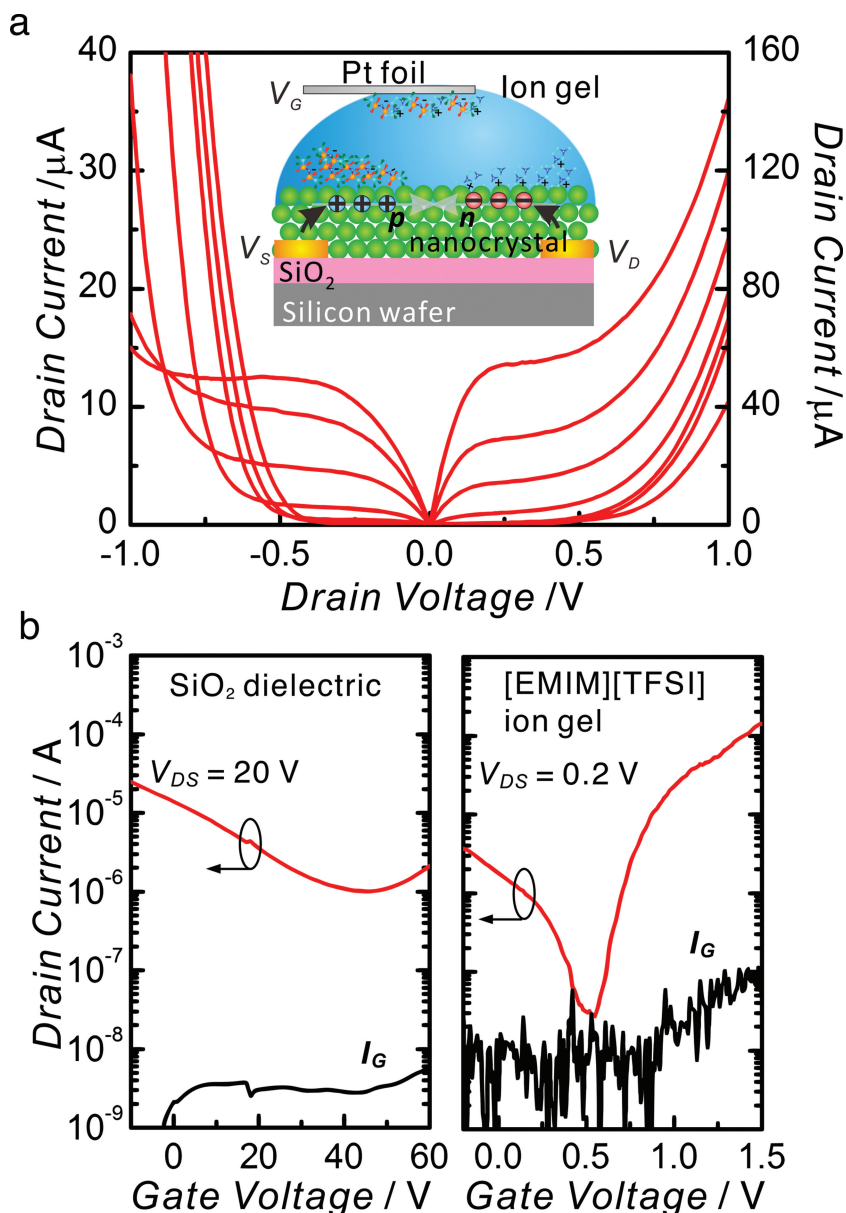


Figure 4. (a) p-channel and n-channel I_D - V_D output characteristics of ion-gel-gated ambipolar FET of PbS colloidal nanocrystal. V_G is applied from 0.2 V to -1.0 V for p-channel and from -0.2 V to 1.0 V for n-channel with 0.2 V increment. V_D sweep is 10 mV s^{-1} . (inset) Schematic of the ion-gel-gated transistor. (b) Comparison of the n-channel I_D - V_G transfer characteristics between conventional SiO_2 (left) and [EMIM][TFSI] ion-gel (right) gateings. The black curves show the I_G leak current vs V_G for both devices. In both devices the I_G leak current is minimal in comparison to the I_D drain current. The V_G sweep is 10 mV s^{-1} .

the morphology of PbS NC film deposited on the untreated SiO_2 surface and cross-linked using 3MPA molecules. The film consist of two monolayers of NC assembly, where the second monolayer is filling the cracks resulting from the first ligand exchange process. The average thickness of the film is 9.8 nm, which is in agreement with its composition: two monolayers of NCs with 3.6 nm diameter and the surrounding ligands (3MPA molecular length = 0.6 nm). The AFM image shows that the 3MPA treated PbS film is homogeneous and crack free, and therefore suitable for devices fabrication.

Figure 3b shows the I_D - V_D output characteristics of these devices for both the p-channel and n-channel operations. It is clear that the thicker PbS NC layer gave higher I_D for both holes and electrons. A clear linear and saturation regimes are observed in all devices with different thicknesses. Therefore, we extract the values of charge carrier mobilities from the linear regime using Equation 1, as well as from the saturation regime using the following formula,

$$\mu_{sat} = \frac{2L_C}{W_C} \frac{1}{C} \left(\frac{\partial I_D^{1/2}}{\partial V_G} \right)^2 \quad (2)$$

The thickness-dependent charge carrier mobility values for holes and electrons extracted from both linear and saturation regimes are shown in Figure 3c. Varying the number of NC layers, the values of charge carrier mobility increases. The value of the mobility in the devices with 10 MLs of NCs is more than twice the one of the device with only 2 MLs of NCs. This carrier mobility enhancement indicates that charge carrier transport in NC films is highly influenced by the number of percolation paths, which is proportional to the film thickness. The increase in the carrier mobility values starts to saturate after 7 MLs at around $5.8 \times 10^{-3} \text{ cm}^2 \text{ V}^{-1} \text{ s}^{-1}$ and $6.2 \times 10^{-2} \text{ cm}^2 \text{ V}^{-1} \text{ s}^{-1}$ for holes and electron, respectively. These results are in good agreement with most reports on organic thin-film transistor devices,^[31,32] in which the first 5-10 molecular monolayers have the biggest influence in forming the effective charge transport percolation path.

The last effort made towards the optimization of PbS based FET is the utilization of an EDL gate. Despite the interesting results obtained by using the BG/TC device configuration, the value of voltage that need to be applied to reach the saturation is still too high in the perspective of practical applications. The EDL technique allows to reach high carrier mobility by applying very low voltage.

Ion gel of 1-ethyl-3-methylimidazolium bis(trifluoromethylsulfonyl)imide ([EMIM][TFSI]) was deposited on top of the channel of a BG/BC substrate (inset of Figure 4a). The device channel consisted of 5 MLs of PbS nanocrystals. The [EMIM][TFSI] ion gel has been known to be as effective as ionic liquid in forming a highly capacitive EDL under an electric field. Higher values of carrier mobilities are expected because the ion gel allows a consistent increase in carrier density at the interface between the PbS NC film and the ion gel.

Ambipolar transport characteristics are observed in the PbS NC ion-gel-gated transistor with clear carrier accumulation mode (both for the linear and saturation regime) by applying a

very small values of V_D and V_G (up to ± 1 V). Figure 4a shows the I_D - V_D output characteristics of the ion-gel-gated FETs in p-channel and n-channel operation. In the lower V_D regime ($|V_D| < 0.25$ V), the I_D value linearly increases before saturating. The saturation behavior was observed for both holes and electrons, with no degradation. At higher V_D , indications of secondary-carrier transport, i.e. electrons for p-channel operation and holes for n-channel operation, was observed. In this (ambipolar) regime, both holes and electrons are involved in the transport process, but they are travelling in opposite directions. The co-existence of electrons and holes in the channel has great potential for the realization of ambipolar light-emitting transistors.^[33,34] Figure 4b shows the comparison of I_D - V_G transfer characteristics between the ion-gel-gated transistor and the identical device when gated by SiO_2 . The on/off ratio of the ion-gel-gated transistor is 10^4 , three orders of magnitude higher than the corresponding conventional transistor. This on/off ratio value is achieved because of the off-current decrease and the increase of on-current. The holes and electrons subthreshold swing values are 300 mV/decade and 110 mV/decade, respectively. These values are significantly better than the values obtained in conventional PbS nanocrystal device, which are of the order of 10 V/decade. The subthreshold swing values of the ion-gel-gated transistor, in particular for electrons, are close to the ideal value of a trapless transistor, 66 mV/decade.^[35] It is well known that the on/off ratio of PbS nanocrystal transistors, particularly those using 3MPA ligands, is low due to high off-current.^[23,24] Our results show that the use of ion-gel gate of dispersed ionic liquid can effectively deplete the conduction channel of the transistors, better than the SiO_2 gate as well as of the polymer electrolyte gate. While the reason of the high "off current" in 3MPA-treated films is still unknown, ion gels provide a strategy to achieve effective charge depletion due to the effective trap filling.

To extract the values of the charge carrier mobilities in this ion-gel gated ambipolar FET, first we need to measure the capacitance-voltage characteristics of the ion gel on the PbS NC films in the same conditions of the transistor. From the measurements, the V_G -dependent charge carrier density (n) is calculated using $n = (1/e)C \cdot dV_G$,^[36] where e is the elemental charge and C is the measured capacitance. We accumulated up to $0.5 \times 10^{14} \text{ cm}^{-2}$ at $V_G = \pm 1.5$ V for both electrons and holes. These values are more than one order of magnitude higher than the value for the accumulated charge in the corresponding conventional SiO_2 gated device, $C_{230 \text{ nm}} \approx 15 \text{ nF cm}^{-2} \rightarrow n(60 \text{ V}) \approx 5.63 \times 10^{12} \text{ cm}^{-2}$. The density of the nanocrystal arrangement in the first layer is estimated to be $6.55 \times 10^{12} \text{ cm}^{-2}$ by considering the *hcp*-like packing density of the PbS nanocrystal assembly.^[4] If the accumulated charge carriers spread throughout the whole thickness (5ML) of the transistor, each nanocrystal is doped with almost two charge carriers. The carrier mobilities are calculated using:

$$\mu = \frac{L_C}{W_C} \frac{1}{e V_{DS}} \frac{I_D}{n} \quad (3)$$

which is derived from Ohm's law, where n is the value of the V_G -dependent carrier density. Electron mobility as high as $1.91 \text{ cm}^2 \text{ V}^{-1} \text{ s}^{-1}$ and hole mobility up to $0.15 \text{ cm}^2 \text{ V}^{-1} \text{ s}^{-1}$ are

achieved. These mobility values are more than two orders of magnitude higher than those obtained from the conventional SiO_2 -gated device in the identical structure. To our knowledge, these values are among the highest reported for solution-processed PbS nanocrystal transistors and they are particularly remarkable since no high temperature annealing/sintering treatments ($\geq 200^\circ \text{C}$)^[10,37] were performed.

In conclusion, we have successfully improved the charge carrier mobilities in ambipolar FET of PbS NCs as much as 5 order of magnitudes by combining a systematic approach to optimize the selection of coupling ligand molecules and the device structure. The use of ion gel gating allows filling the charge carrier traps, resulting in an improvement of the on/off ratio of the device while operating it at very low driving voltage. The high ($1.91 \text{ cm}^2 \text{ V}^{-1} \text{ s}^{-1}$ for electrons and $0.15 \text{ cm}^2 \text{ V}^{-1} \text{ s}^{-1}$ for holes) charge carrier mobilities obtained indicate that PbS colloidal nanocrystals are relevant not only for solar cells applications, but also in the other electronics and optoelectronics devices. The achieved carrier mobility values are the record highest for non-sintered PbS nanocrystal thin films. The very high carrier mobility in this ambipolar transistors opens up the possibility to investigate the intrinsic properties of PbS colloidal nanocrystal which are related to the transport process, including confirming the band-like transport findings from the spectroscopic and solar cell measurements.

Experimental Section

Device fabrication: All device fabrication and measurements were performed inside an N_2 -filled glovebox. The transistors were fabricated by a layer-by-layer (LbL) sequential spin-coating technique with ligand exchange process performed on each layer. For each layer, 5 mg/mL solution of PbS in chloroform were spin-coated at 4000 rpm, to form a single monolayer film of the nanocrystals. Subsequently, the PbS film was soaked in a solution of the different ligands (3-mercaptopropionic acid (Sigma Aldrich), benzenedithiol (TCI), ethanedithiol (Sigma Aldrich)) in methanol for 30 s to replace the insulating oleic acid. The substrate was then spin-dried at 4000 rpm to remove the residual solution. The morphology of the films was determined by tapping mode AFM.

For the bottom gate bottom contact transistor (BG/BC) configuration, we used 230 nm SiO_2/Si wafer with lithographically patterned interdigitated electrodes (30 nm Au), on which the PbS nanocrystal film was deposited. The channel length of these FET devices was 20 μm and their channel width was 10 mm. For bottom-gate top-contact (BG/TC) configuration, 30 nm Au was evaporated through shadow mask on the PbS nanocrystal film deposited on 230 nm SiO_2/Si wafer. The channel width of these BG/TC devices was 10 mm with channel length of 100 μm . The channel dimension of the ion-gel gated FETs was identical to the one of the BG/BC transistor configuration.

Ion gel of 1-ethyl-3-methylimidazolium bis(trifluoromethylsulfonyl) imide ([EMIM][TFSI]) was synthesized by dispersing the ionic liquids into polystyrene-*b*-polymethyl(meth)acrylate-*b*-polystyrene block co-polymer matrix using ethyl-acetate as solvent. From the homogeneous solution, the solvent is evaporated by using a vacuum rotary evaporator in order to reach the intended gel. The ion gel is then dropped on the transistor channel and a Pt foil is used as the gate electrode.

Device measurements: Transistor measurements were performed by using a probe station inside a nitrogen-filled glovebox under dark conditions at room temperature. The transistor characteristics were acquired by an Agilent E5270B semiconductor parameter analyzer. The electrochemical properties of the ion gel were measured by an electrochemical impedance analyzer (Bio Logic, SP-200).

Acknowledgements

This research is partially funded by The European Research Council Starting Grant (No. 306983) "Hybrid solution processable materials for opto-electronic devices" (ERC-HySPOD). The authors would like to acknowledge L. H. Lai for discussion and F. van der Horst, A. F. Kamp, J. G. Holstein, and R. Gooijaarts for technical support.

Received: December 8, 2012

Revised: February 22, 2013

Published online: April 12, 2013

- [1] C. B. Murray, C. R. Kagan, M. G. Bawendi, *Ann. Rev. Mater. Sci.* **2000**, *30*, 545–610.
- [2] D. V. Talapin, J.-S. Lee, M. V. Kovalenko, E. V. Shevchenko, *Chem. Rev.* **2010**, *110*, 389–458.
- [3] K. Szendrei, W. Gomulya, M. Yarema, W. Heiss, M. A. Loi, *Appl. Phys. Lett.* **2010**, *97*, 203501.
- [4] K. Szendrei, M. Speirs, W. Gomulya, D. Jarzab, M. Manca, O. V. Mikhnenko, M. Yarema, B. J. Kooi, W. Heiss, M. A. Loi, *Adv. Funct. Mater.* **2012**, *22*, 1598–1605.
- [5] A. H. Ip, S. M. Thon, S. Hoogland, O. Voznyy, D. Zhitomirsky, R. Debnath, L. Levina, L. R. Rollny, G. H. Carey, A. Fischer, K. W. Kemp, I. J. Kramer, Z. Ning, A. J. Labelle, K. W. Chou, A. Amassian, E. H. Sargent, *Nat. Nanotechnol.* **2012**, *7*, 577–582.
- [6] G. Konstantatos, I. Howard, A. Fischer, S. Hoogland, J. Clifford, E. Klem, L. Levina, E. H. Sargent, *Nature* **2006**, *442*, 180–183.
- [7] K. Szendrei, F. Cordella, M. V. Kovalenko, M. Böberl, G. Hesser, M. Yarema, D. Jarzab, O. V. Mikhnenko, A. Gocalinska, M. Saba, F. Quochi, A. Mura, G. Bongiovanni, P. W. M. Blom, W. Heiss, M. A. Loi, *Adv. Mater.* **2009**, *21*, 683–687.
- [8] T. Rauch, M. Böberl, S. F. Tedde, J. Fürst, M. V. Kovalenko, G. Hesser, U. Lemmer, W. Heiss, O. Hayden, *Nat. Photonics* **2009**, *3*, 332–336.
- [9] L. Sun, J. J. Choi, D. Stachnik, A. C. Bartnik, B.-R. Hyun, G. G. Malliaras, T. Hanrath, F. W. Wise, *Nat. Nanotechnol.* **2012**, *7*, 369–373.
- [10] J.-S. Lee, M. Kovalenko, J. Huang, D. Chung, D. Talapin, *Nat. Nanotechnol.* **2011**, *6*, 348–352.
- [11] H. Minemawari, T. Yamada, H. Matsui, J. Tsutsumi, S. Haas, R. Chiba, R. Kumai, T. Hasegawa, *Nature* **2011**, *475*, 364–367.
- [12] J. Soeda, Y. Hirose, M. Yamagishi, A. Nakao, T. Uemura, K. Nakayama, M. Uno, Y. Nakazawa, K. Takimiya, J. Takeya, *Adv. Mater.* **2011**, *23*, 3309–3314.
- [13] M. H. Zarghami, Y. Liu, M. Gibbs, E. Gebremichael, C. Webster, M. Law, *ACS Nano* **2010**, *4*, 2475–2485.
- [14] J. J. Choi, J. Luria, B.-R. Hyun, A. C. Bartnik, L. Sun, Y.-F. Lim, J. A. Marohn, F. W. Wise, T. Hanrath, *Nano Lett.* **2010**, *10*, 1805–1811.
- [15] D. V. Talapin, *Science* **2005**, *310*, 86–89.
- [16] D. Zhitomirsky, I. Kramer, A. Labelle, A. Fischer, R. Debnath, J. Pan, O. Bakr, E. Sargent, *Nano Lett.* **2012**, *12*, 1007–1012.
- [17] O. Voznyy, D. Zhitomirsky, P. Stadler, Z. Ning, S. Hoogland, E. H. Sargent, *ACS Nano* **2012**, *6*, 8448–8455.
- [18] D. Zhitomirsky, M. Furukawa, J. Tang, P. Stadler, S. Hoogland, O. Voznyy, H. Liu, E. H. Sargent, *Adv. Mater.* **2012**, *24*, 6181–6185.
- [19] H. Shimotani, H. Asanuma, A. Tsukazaki, A. Ohtomo, M. Kawasaki, Y. Iwasa, *Appl. Phys. Lett.* **2007**, *91*, 082106.
- [20] H. Yuan, H. Shimotani, A. Tsukazaki, A. Ohtomo, M. Kawasaki, Y. Iwasa, *Adv. Funct. Mater.* **2009**, *19*, 1046–1053.
- [21] H. Hwang, Y. Iwasa, M. Kawasaki, B. Keimer, N. Nagaosa, Y. Tokura, *Nat. Mater.* **2012**, *11*, 103–113.
- [22] T. P. Osedach, N. Zhao, T. L. Andrew, P. R. Brown, D. D. Wanger, D. B. Strasfeld, L.-Y. Chang, M. G. Bawendi, V. Bulovi, *ACS Nano* **2012**, *6*, 3121–3127.
- [23] K. S. Jeong, J. Tang, H. Liu, J. Kim, A. W. Schaefer, K. Kemp, L. Levina, X. Wang, S. Hoogland, R. Debnath, L. Brzozowski, E. H. Sargent, J. B. Asbury, *ACS Nano* **2012**, *6*, 88–99.
- [24] J. Tang, K. W. Kemp, S. Hoogland, K. S. Jeong, H. Liu, L. Levina, M. Furukawa, X. Wang, R. Debnath, D. Cha, K. W. Chou, A. Fischer, A. Amassian, J. B. Asbury, E. H. Sargent, *Nat. Mater.* **2011**, *10*, 765–771.
- [25] E. J. D. Klem, H. Shukla, S. Hinds, D. D. MacNeil, L. Levina, E. H. Sargent, *Appl. Phys. Lett.* **2008**, *92*, 212105.
- [26] K. P. Puntambekar, P. V. Pesavento, C. D. Frisbie, *Appl. Phys. Lett.* **2003**, *83*, 5539–5541.
- [27] D. Natali, M. Caironi, *Adv. Mater.* **2012**, *24*, 1357–1387.
- [28] S. Scheinert, G. Paasch, *J. Appl. Phys.* **2009**, *105*, 014509.
- [29] S. Shankara Narayanan, S. S. Sinha, P. K. Verma, S. K. Pal, *Chem. Phys. Lett.* **2008**, *463*, 160–165.
- [30] S. Z. Bisri, T. Takenobu, T. Takahashi, Y. Iwasa, *Appl. Phys. Lett.* **2010**, *96*, 183304.
- [31] R. Ruiz, A. Papadimitratos, A. C. Mayer, G. G. Malliaras, *Adv. Mater.* **2005**, *17*, 1795–1798.
- [32] S. Fabiano, C. Musumeci, Z. Chen, A. Scandurra, H. Wang, Y.-L. Loo, A. Facchetti, B. Pignataro, *Adv. Mater.* **2012**, *24*, 951–956.
- [33] S. Z. Bisri, T. Takenobu, K. Sawabe, S. Tsuda, Y. Yomogida, T. Yamao, S. Hotta, C. Adachi, Y. Iwasa, *Adv. Mater.* **2011**, *23*, 2753–2758.
- [34] S. Z. Bisri, K. Sawabe, M. Imakawa, K. Maruyama, T. Yamao, S. Hotta, Y. Iwasa, T. Takenobu, *Sci. Rep.* **2012**, *2*, 985.
- [35] S. M. Sze, K. K. Ng, *Physics of Semiconductor Devices*, John Wiley & Sons, **2007**.
- [36] M. Kang, J. Lee, D. Norris, C. Frisbie, *Nano Lett.* **2009**, *9*, 3848–3852.
- [37] J.-H. Choi, A. T. Fafarman, S. J. Oh, D.-K. Ko, D. K. Kim, B. T. Diroll, S. Muramoti, J. G. Gillen, C. B. Murray, C. R. Kagan, *Nano Lett.* **2012**, *12*, 2631–2638.